Polyoxometalate-Supported Copper(I)−Pyrazole Complex: Unusual Stability, Geometrical Isomers, Organic Transformation, and Computation

Neeraj Kumar Mishra, Deepak Bansal, and Sabbani Supriya*

Read Online

ACCESS | Metrics & More | Article Recommendations | SI Supporting Information

ABSTRACT: We have described the synthesis and characterization of a polyoxometalate (POM)-supported copper(I)−pyrazole complex, $[Cu^I(C_{15}H_{12}N_2)_2]$ $[PW_{12}O_{40}\{Cu^I(C_{15}H_{12}N_2)_2\}_2]\cdot CH_3OH$ (**1**). There are three Cu-(I)−pyrazole coordination complexes in compound **1**, out of which two are supported by the $\{PW_{12}O_{40}\}^{3-}$ Keggin POM by coordinate covalent bonds from the POM surface through oxygen donors to the Cu(I) centers of two Cu(I) complexes and one remains uncoordinated to the POM surface, acting as a cationic complex species in the crystals of **1**. The POM-coordinated Cu(I) complexes have a T-shaped geometry, and the uncoordinated Cu(I) complex is a linear one. During the solvothermal synthesis of compound **1**, remarkably, the associated 1,5-diphenylpyrazole ligand is formed from cinnamaldehyde phenylhydrazone through oxidative cyclization at the cost of Cu(II) reduction to Cu(I), and then, these two (copper(I) and pyrazole ligand) form the coordination complex. Compound **1** undergoes desolvation on heating the single crystals of compound **1** at 55 °C in the aerial atmosphere with the formation of the desolvated compound $[Cu^I(C_{15}H_{12}N_2)_2][PW_{12}O_{40}\{Cu^I(C_{15}H_{12}N_2)_2\}_2]$ (**2**). Interestingly, when an aqueous suspension of compound **1** is bubbled with O_2 gas at room temperature, it undergoes solid-to-solid transformation, resulting in the formation of the compound $[Cu^I(C_{15}H_{12}N_2)_2]_3[PW_{12}O_{40}]$ (**3**). Compounds **1**, **2**, and **3** have been characterized by routine spectral analyses (including cyclic voltammetry and X-ray photoelectron spectroscopy (XPS) studies) and unambiguously by single-crystal X-ray crystallography. We have performed density functional theory (DFT) calculations on compound **1** to understand the rationale of its unusual stability toward oxidation.
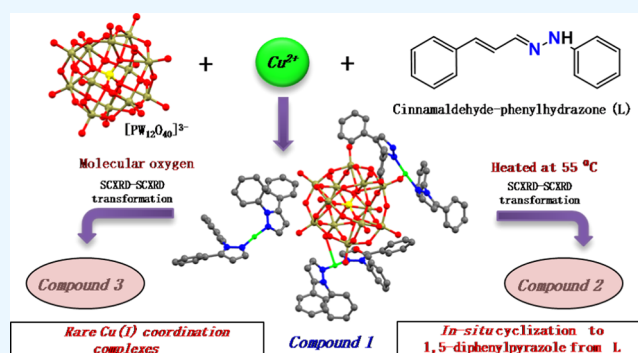
INTRODUCTION

Polyoxometalates (POMs) are a subset of metal oxides, consisting of metal−oxo anionic clusters of early transition metals, mainly V, W, Mo, *etc.*[1−3] POMs are formed because of the required ionic size of these early transition metal ions and their good acceptability of π electrons from oxygen. These metal ions in their resulting POMs are called addenda atoms. The POM clusters show diverse topologies, and the relevant compounds exhibit their unique intrinsic properties, such as Lewis's acidity, reversible redox behavior in electrochemistry,[4,5] magnetism,[6,7] and catalysis.[8−14] Modern polyoxometalate (POM) chemistry research includes mainly designing POM-based multifunctional materials with the incorporation of organic molecules/metal coordination complexes in the POM matrix.[15] The POM-based organic−inorganic hybrids are broadly classified into two classes. Class I consists of the hybrids that show the electrostatic, H-bonding, and van der Waals interactions between the POM cluster anion and organic cation/metal coordination complex cation.[16] Class II hybrids include compounds with covalent interactions between the

POM cluster anion and transition metal complex cation, for example, the POM cluster anion coordinates to the metal ion through its terminal oxygen or bridging oxygen.[17−20] Both classes of these inorganic−organic hybrid compounds show diverse applications. In a study by Zhao et al., Keggin-type polyoxoanions and Cu(II)-2,2′-bpy complex cations form a class I hybrid system, which can be applied for the photodegradation of rhodamine B dye.[21] Hu et al. have reported inorganic−organic hybrids containing Keggin polyoxometalate-supported Ag(I)-amino-pyrimidine coordination complexes (class II hybrid system) and studied their catalytical properties toward the cyanosilylation of carbonyl compounds.[22] Das and co-workers have demonstrated electro-

catalytic water oxidation using the class II system of $[HCo^{II}W_{12}O_{40}]^{5-}$-supported Ni(II)-bipyridine complexes.[23] In the design of class II POM-based hybrid materials, it is important to choose a POM that consists of sufficient charge density at the terminal/bridging oxygen atoms along with a metal coordination complex with an appropriate organic ligand that promotes the formation of coordinate covalent bonding between the metal complex and the POM anion.[24−26] Among the POM-supported transition metal complexes, POM-supported Cu(I) coordination complexes are rarely known. In general, the mononuclear copper(I) coordination complexes are scarcely reported in the literature. Usually, copper(I) complexes undergo oxidation to copper(II) on exposure to molecular oxygen/air. Sorrell et al. have reported stable mononuclear copper(I) complexes with nitrogen donor tripodal ligands.[27] There are reports on Cu(I) complexes emphasizing their photophysical properties;[28−35] in many of these compounds, the coordination environment of the copper(I) ion influences the metal-to-ligand charge transfer (MLCT) transitions.

In the present work, we have reported a rare system of POM-supported Cu(I) coordination complex, $[Cu^{I}(C_{15}H_{12}N_2)_2]$ $[PW_{12}O_{40}\{Cu^{I}(C_{15}H_{12}N_2)_2\}_2]\cdot CH_3OH$ (1). The formation of compound 1 is accompanied by the oxidative cyclization of cinnamaldehyde phenylhydrazone to 1,5-diphenylpyrazole, which coordinates to the Cu(I) center in 1. The compound 1 crystals on heating at 55 °C under the atmospheric aerial conditions get desolvated and transformed into the compound $[Cu^{I}(C_{15}H_{12}N_2)_2]$-$[PW_{12}O_{40}\{Cu^{I}(C_{15}H_{12}N_2)_2\}_2]$ (2). Interestingly, compound 1 crystals undergo transformation in an oxygen atmosphere, forming the compound $[Cu^{I}(C_{15}H_{12}N_2)_2]_3[PW_{12}O_{40}]$ (3), a geometrical isomer of compound 2. Compounds 1, 2, and 3 have unambiguously been characterized by single-crystal X-ray crystallography. The formation of compounds 2 and 3 from compound 1 in an oxygen atmosphere strongly indicates that Cu(I) compound 1 is unusually stable toward oxidation. We have performed density functional theory (DFT) calculations to understand the unusual stability of the title copper(I) complex toward aerial oxidation.

RESULTS AND DISCUSSION

Synthesis. The pertinent synthesis involves phosphotungstic acid, copper(II) acetate, and a cinnamaldehyde phenylhydrazone ligand, resulting in golden yellow single crystals of $[Cu^{I}(C_{15}H_{12}N_2)_2]$ $[PW_{12}O_{40}\{Cu^{I}(C_{15}H_{12}N_2)_2\}_2]\cdot CH_3OH$ (1). Surprisingly, compound 1 contains the ligand 1,5-diphenylpyrazole coordinated to the Cu(I) center, not the ligand cinnamaldehyde phenylhydrazone used in the synthesis. Thus, the important feature of the present synthesis is the oxidative cyclization of cinnamaldehyde phenylhydrazone to 1,5-diphenylpyrazole (Figure 1) and reduction of Cu(II) to Cu(I). The oxidatively cyclized 1,5-diphenylpyrazole coordinates to the Cu(I) center in compound 1. The POM unit $[PW_{12}O_{40}]^{3-}$ coordinates to two such Cu(I)−pyrazole complexes, resulting in T-shape geometry around the Cu(I) center. The crystal structure of compound 1 also consists of one Cu(I)−pyrazole complex, which is not coordinated to the POM unit, and two solvent methanol molecules. The oxidative cyclization of cinnamaldehyde phenylhydrazone (Figure 1) is worth mentioning, which demonstrates intramolecular C−N bond formation via oxidation of the C−H bond that plays an
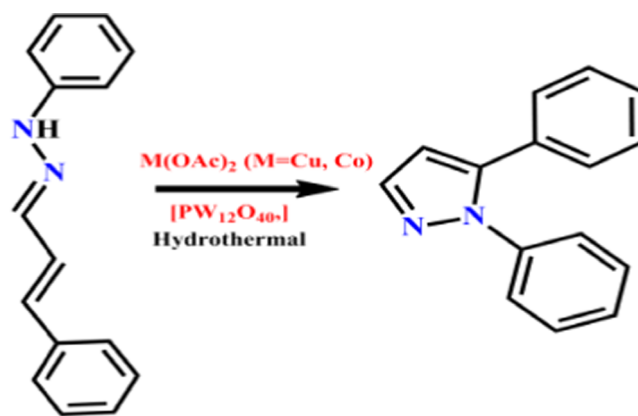

Figure 1. Oxidative cyclization of cinnamaldehyde phenylhydrazone to 1,5-diphenylpyrazole during the solvothermal synthesis of compound 1.

important role in nitrogen-containing heterocyclic systems and in related chemistry.

The transition metal-catalyzed C−H bond functionalization followed by C−N bond formation represents one of the most versatile and practical approaches for the formation of nitrogen-containing functional groups. Particularly, the copper-catalyzed oxidative C−H bond functionalization for the C−N bond formation is one of the green synthetic routes.[36] The oxidative cyclization of hydrazones, catalyzed by copper acetate $(Cu(OAc)_2)$, is reported in the literature.[37] The mechanistic studies of the synthesis of pyrazole from aryl hydrazones catalyzed by $Cu(OAc)_2$ involve the formation of the Cu−N adduct and then a metallacycle[38] followed by reductive elimination[39] to give the corresponding pyrazole product. We believe that in the present system, because of the presence of polyoxometalate, which is coordinated to the Cu(II) center during the cyclization of hydrazone to pyrazole, the reductive elimination is not complete, and the Cu(II) center is reduced to Cu(I) instead of going to Cu(0); thus, the cyclized pyrazole ligand does not detach from the Cu(I) center as found in isolated compounds 1 and 2. Hence, polyoxometalate in the present study plays an important role in the stabilization of the Cu(I)−pyrazole coordination complex.

It is important to note that 1,5-diphenylpyrazole stabilizes the Cu(I) center in compound 1. Usually, Cu(I) compounds easily undergo oxidation and form the corresponding Cu(II) compounds. However, this is not the case for the title compound 1. When the single crystals of compound 1 are heated at 55 °C under aerial conditions, they undergo desolvation with the formation of the desolvated compound $[Cu^{I}(C_{15}H_{12}N_2)_2][PW_{12}O_{40}\{Cu^{I}(C_{15}H_{12}N_2)_2\}_2]$ (2) but without any redox reaction, as shown in eq 1. On the other hand, when the single crystals of compound 1 are exposed to pure oxygen at room temperature, compound 1 undergoes transformation (eq 2), leading to the formation of compound 3.

Desolvation

$$[Cu^{I}(C_{15}H_{12}N_2)_2][PW_{12}O_{40}\{Cu^{I}(C_{15}H_{12}N_2)_2\}_2]$$
$$\cdot CH_3OH\ (\mathbf{1}) + \text{heated at 55 °C in air}$$
$$\rightarrow [Cu^{I}(C_{15}H_{12}N_2)_2][PW_{12}O_{40}\{Cu^{I}(C_{15}H_{12}N_2)_2\}_2]\ (\mathbf{2})$$
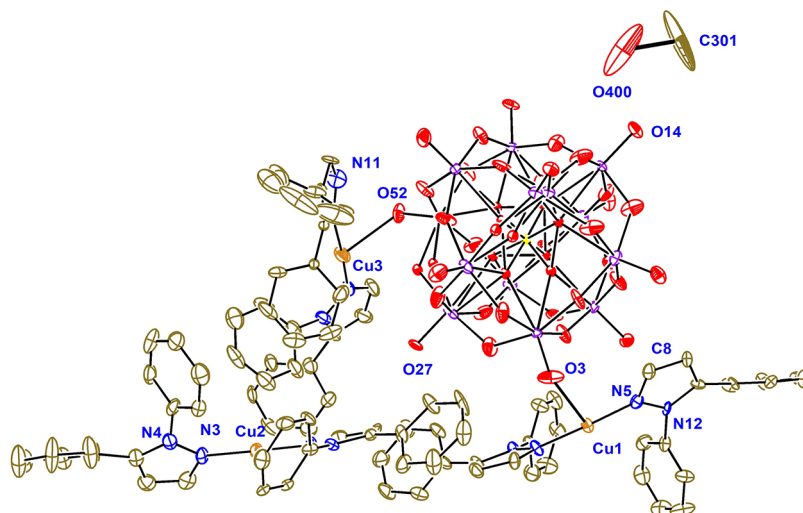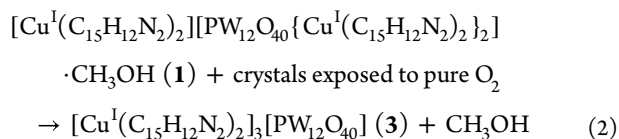$$+ CH_3OH \tag{1}$$
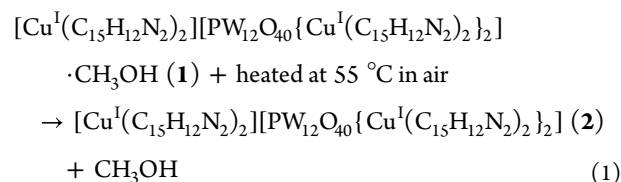
Figure 2. ORTEP diagram of the full molecule of **1** with the ellipsoid drawn at 50% probability viewed down the crystallographic *b*-axis. Color scheme: W, purple; P, yellow; O, red; C, olive green; N, blue; and Cu, brown.

Geometrical isomer

$$[Cu^I(C_{15}H_{12}N_2)_2][PW_{12}O_{40}\{Cu^I(C_{15}H_{12}N_2)_2\}_2]$$

$$\cdot CH_3OH\ (\mathbf{1}) + \text{crystals exposed to pure } O_2$$

$$\rightarrow [Cu^I(C_{15}H_{12}N_2)_2]_3[PW_{12}O_{40}]\ (\mathbf{3}) + CH_3OH \quad (2)$$

(Compounds **1** and **2** are geometrical isomers to each other).

It is worth stating that compound **1** is unusually stable in the aerial atmosphere even at a temperature more than 50 °C. It clearly indicates that the 1,5-diphenylpyrazole ligand might have low-lying antibonding molecular orbitals that can accept electrons from the coordinated Cu(I) center by backdonation to stabilize the system (*vide infra*, Crystallography and DFT Calculations).

Compounds $[Cu^I(C_{15}H_{12}N_2)_2][PW_{12}O_{40}\{Cu^I\text{-}(C_{15}H_{12}N_2)_2\}_2]$ (**2**) and $[Cu^I(C_{15}H_{12}N_2)_2]_3[PW_{12}O_{40}]$ (**3**) are geometrical isomers to each other. The geometrical isomerization, in the present work, involves detachment of the Cu(I) complexes from the POM through breaking of the Cu−O bond. It is difficult to place the mechanistic insights of this isomerization because a Cu(I) complex, which is supposed to be susceptible to oxidation in an oxygen environment, does not get oxidized (referring to bond valence sum calculations and X-ray photoelectron spectroscopy (XPS) results); instead, bond breaking occurs, leading to geometrical isomerization. We speculate that in compounds **1** and **2**, the Cu(I)−pyrazole complexes that are coordinated to the terminal oxygen of the POM (T-shaped geometry around the Cu(I) center) are in a strained situation because a Cu(I) coordination complex favors a linear structure (e.g., in compound **3**), rather than a T-shaped structure (referring to compounds **1** and **2**). When compound **1** crystals are exposed to oxygen, we believe that oxygen competes with the POM and detaches the POM from the Cu(I)−pyrazole coordination complex. O₂ coordination to the Cu-center is unlikely because the resulting linear Cu(I)−pyrazole complex is more stable. At this stage, the coordinated Cu(I)−pyrazole complex shows enormous stability toward oxidation due to the backbonding i.e., metal donates π-electron density to the pyrazole ligand. This speculation can be supported by DFT calculations of compound **1** (*vide infra*).

Crystallography.[40,41] Compound **1** crystallizes in the space group *P$\bar{1}$* with two formula units per unit cell, in which the asymmetric unit contains a formula unit of Keggin ion with two T-shaped copper(I) pyrazole complexes coordinated to the POM cluster, one linear copper(I) mononuclear complex with two 1,5-diphenylpyrazole ligands, and one methanol molecule as shown in its formula, $[Cu^I(C_{15}H_{12}N_2)_2]$-$[PW_{12}O_{40}\{Cu^I(C_{15}H_{12}N_2)_2\}_2]\cdot CH_3OH$ (**1**). The thermal ellipsoidal diagram of compound **1** is shown in Figure 2.

The Keggin POM cluster anion contains a central tetrahedral phosphate ion, while the 12{WO₆} octahedra are placed on the 12 vertices of a regular cuboctahedron, equidistant from the central phosphorus atom. The charge on the Keggin anion has been balanced with the three cuprous complexes, which is confirmed by bond valence sum (BVS) calculations.[42] Weak intermolecular hydrogen bonding interactions can be observed between the pyrazole and Keggin anion *via* N−H···O (Keggin) hydrogen bonds (D−A distance 3.3 Å). CH$_\pi$···O (Keggin) interactions are also present in the crystal structure. The two copper centers (Cu1 and Cu3) of compound **1** adopt T-shaped geometries with coordination to teh terminal oxygen of Keggin and N atoms of two different pyrazoles. Thus, the terminal oxygen atom of the Keggin POM anion is roughly perpendicular to the pyrazole-*N*−Cu(I)−*N*-pyrazole linear arrangement. The third cuprous atom (Cu2) has a linear geometry with coordination to two pyrazole units. Crystallographic parameters (Table S1) and hydrogen bonding parameters (Table S2) for compound **1** are presented in the Supporting Information.

Desolvation and Geometrical Isomerism. When the crystals of the compound $[Cu^I(C_{15}H_{12}N_2)_2]$-$[PW_{12}O_{40}\{Cu^I(C_{15}H_{12}N_2)_2\}_2]\cdot CH_3OH$ (**1**) are heated to 55 °C under aerial conditions for 5 h, they undergo desolvation with the formation of the compound $[Cu^I(C_{15}H_{12}N_2)_2]$-$[PW_{12}O_{40}\{Cu^I(C_{15}H_{12}N_2)_2\}_2]$ (**2**). The single-crystal structure analysis of compound **2** shows the *P$\bar{1}$* space group similar to that of compound **1**, but crystallographic parameters of the resulting compound **2** get changed considerably compared to those of compound **1**. It has been observed that the values of *a* and *b* unit cell parameters are increased from 12.88 and 15.74 Å (compound **1**) to 16.64 and 17.47 Å (compound **2**), respectively, while the *c* parameter gets decreased from 28.52
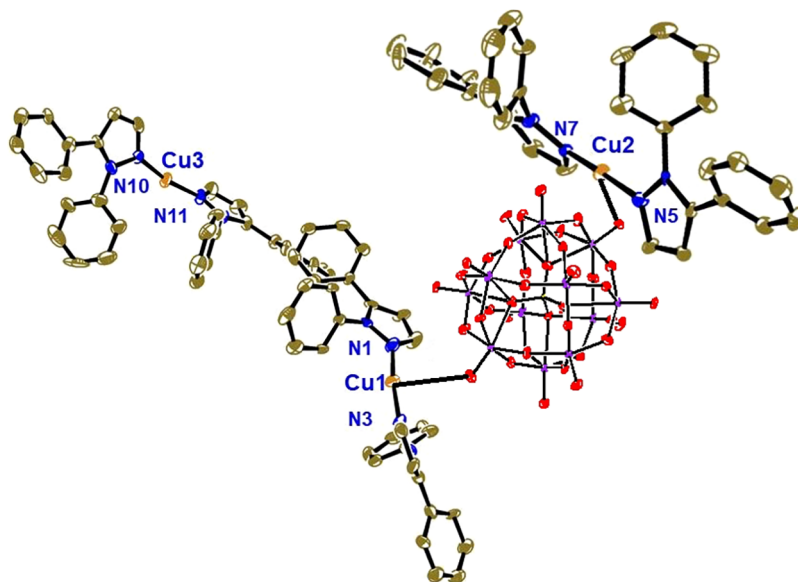
Figure 3. ORTEP diagram of the full molecule of **2** with the ellipsoid drawn at 50% probability, viewed down the crystallographic *a*-axis. Color scheme: W, purple; P, yellow; O, red; C, olive green; N, blue; and Cu, brown.
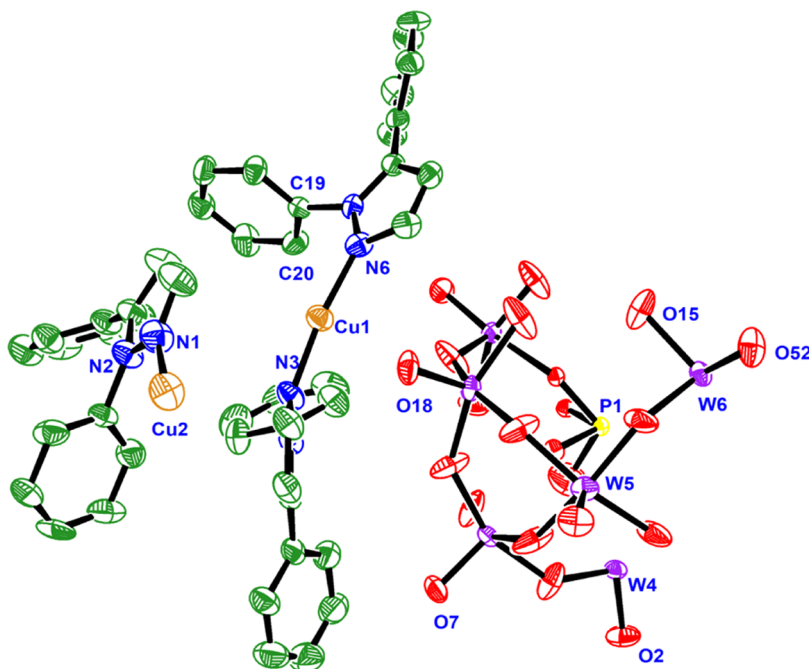

Figure 4. ORTEP diagram of the asymmetric unit of compound **3** with the ellipsoid drawn at 50% probability viewed down the *b*-axis. Color scheme: W, purple; P, yellow; O, red; C, green; N, blue; and Cu, brown.

(compound **1**) to 21.03 Å (compound **2**) on solid-state conversion from compound **1** to compound **2**. During this conversion, due to the loss of solvent molecules, the volume of the unit cell decreases from 5310 Å^3 (compound **1**) to 5243 Å^3 (compound **2**). Otherwise, compounds **1** and **2** are isostructural. Thus, in the crystal structure of compound **2** also, the Keggin POM anion coordinates to two Cu(I) coordination complexes through the terminal oxygen, forming POM-Cu(I)L$_2$ (L = 1,5-diphenylpyrazole), leaving a linear Cu(I)L$_2$ complex (not coordinated POM) as shown in Figure 3.

The linear Cu(I) mononuclear complex is situated comparatively far from the Keggin anion (compound **2**) as compared to that in the crystal structure of compound **1**. No classical hydrogen bonds are found in the crystal structure of compound **2**; however, some CH$_\pi$···O (Keggin) interactions are present between the pyrazole and Keggin in compound **2**. The relevant packing diagram is given in the Supporting Information. The oxidation state of the copper center is found to be +1 from bond valence sum calculations (Table S3). Notably, heat treatment on compound **1** crystals at 55 °C under aerial conditions cannot oxidize Cu(I) to Cu(II).

When the crystals of the compound [Cu^I(C$_{15}$H$_{12}$N$_2$)$_2$]-[PW$_{12}$O$_{40}${Cu^I(C$_{15}$H$_{12}$N$_2$)$_2$}$_2$]·CH$_3$OH (**1**) are suspended in water (compound **1** is not soluble in water) and then exposed to pure molecular oxygen (oxygen gas was purged through the
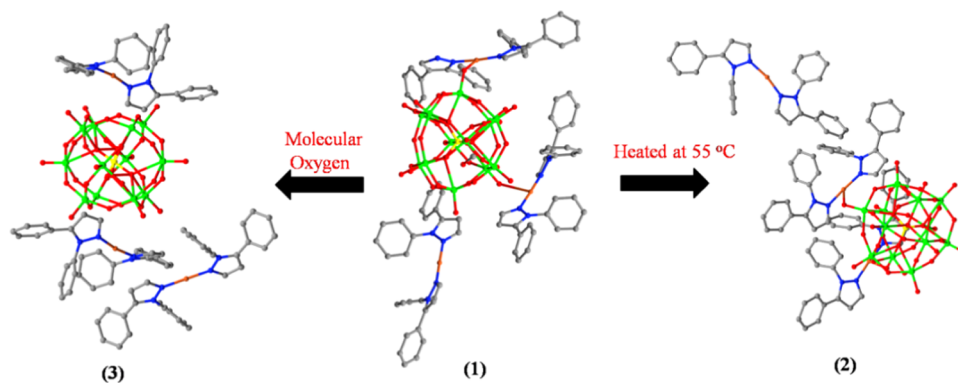
Figure 5. Conversion of the molecular structure of **1** to **2** and **3** by (i) heating the crystals and (ii) exposure of molecular oxygen to the aqueous suspension of **1**. Color scheme: W, green; P, yellow; O, red; C, gray; N, blue; and Cu, brown.

suspension), compound **1** undergoes transformation to the compound $[Cu^I(C_{15}H_{12}N_2)_2]_3[PW_{12}O_{40}]$ (**3**) with three mononuclear linear copper(I) coordination complexes. The asymmetric unit in the crystal structure of compound **3** includes half of the Keggin POM cluster anion and 1.5 molecules of $[Cu^I(C_{15}H_{12}N_2)_2]$. Notably, one of the copper centers and the "P" atom of the Keggin anion are in special positions with half occupancies each. Thus, the formula unit of compound **3** contains a full Keggin cluster anion and three $[Cu^I(C_{15}H_{12}N_2)_2]$ complexes. Importantly, in the crystal structure of compound **3**, all three Cu(I) coordination complexes are not coordinated to the Keggin POM cluster anion unlike what we observed in the crystal structures of compounds **1** and **2**. This means that Cu(I)−O(POM) bond breaking occurs during transformation from compound **1** to compound **3** in the solid state. Thus, compounds **2** and **3** have identical molecular formulas, but they are different in terms of their ligands' arrangement around cuprous centers. In the crystal structure of compound **2**, two $\{Cu^IL_2\}^+$ complex fragments are attached to the POM cluster surface *via* the oxygen atoms of the Keggin anion, and one linear $\{Cu^IL_2\}^+$ complex remains uncoordinated to the Keggin anion. On the other hand, in the crystal structure of compound **3**, none of these $\{Cu^IL_2\}^+$ complex cations are coordinated to the POM cluster (Figure 4). Hence, compounds **2** and **3** can be described as geometrical isomers (to each other) having the same molecular formulas but differing in the arrangement of ligands. In this transformation, molecular oxygen facilitates the breaking of Cu−O(POM) bonds in the solid-to-solid conversion from **1** to **3** instead of oxidizing the Cu(I) center to the Cu(II) center (*vide supra*). The relevant bond valence sum calculations are consistent with the Cu(I) oxidation state. The transformations involving compounds **1**, **2**, and **3** are schematically shown in Figure 5. There is no classical H-bonding situation observed in the crystal structure of compound **3**, and only CH(π)···O interactions are found. Crystal data and structure refinement parameters for compounds **1**, **2**, and **3** are listed in Table S1.

Electrochemistry. The electrochemical experiment of compound **1** was carried out in 0.1 M Na_2SO_4 solution at room temperature in a heterogeneous manner. As shown in Figure 6, an irreversible oxidative response has appeared at +1.13 V *vs* Ag/AgCl as a major oxidation followed by a sudden current surge at around +1.25 V *vs* Ag/AgCl. This irreversible oxidative response is due to the oxidation of Cu(II) to Cu(III), and the appearance of the sudden current surge at around
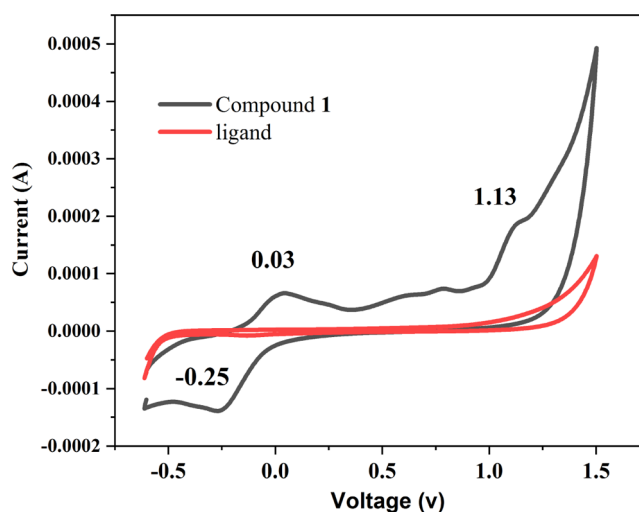

Figure 6. Cyclic voltammograms (CV) for compound **1** and concerned ligand (in 0.1 M Na_2SO_4 solution using a Ag/AgCl reference electrode; scan rate, 100 mV/s).

+1.25 V may be due to the electrocatalytic water oxidation. This assignment is consistent with the relevant literature.[43] The quasi-reversible response at −0.11 V *vs* Ag/AgCl (E_{PC} = −0.25 V and E_{PA} = 0.03 V) can be assigned to the Cu(II)/Cu(I) couple according to the relevant literature.[44] The oxidation of Cu(II) to Cu(III) being irreversible can be explained by hard−soft interactions (Cu^{3+} as an acceptor and hard acid, N as the donor atom and soft base). Similarly, the near-reversible nature of the Cu(II)/Cu(I) couple can be understood by soft−soft interactions (Cu^+ as an acceptor and soft acid, N as the donor atom and soft base).

The control experiment was performed by recording CV of the parent Keggin compound $H_4[PW_{12}O_{40}]\cdot xH_2O$ (Figure S14). This does not show any reductive response for W(VI) centers present in the Keggin compound. Thus, the reductive response observed in the CV profile of compound **1** at −0.11 V *vs* Ag/AgCl is not due to the reduction of the POM unit; rather, it is only due to the Cu(II)/Cu(I) couple.

Spectroscopy. UV−visible (UV−vis) spectroscopy of the synthesized compounds **1** and **2** (5×10^{-5} M) has been performed in *N,N*-dimethylformamide (DMF) solution. The UV−vis spectra of compounds **1** and **2** (Figure 7, left) exhibit intense sharp absorption at around 220 and 270 nm, which are ascribed to $n \rightarrow \pi^*$ transitions of the ligand and O → W charge transfer bands, respectively. The emission properties of
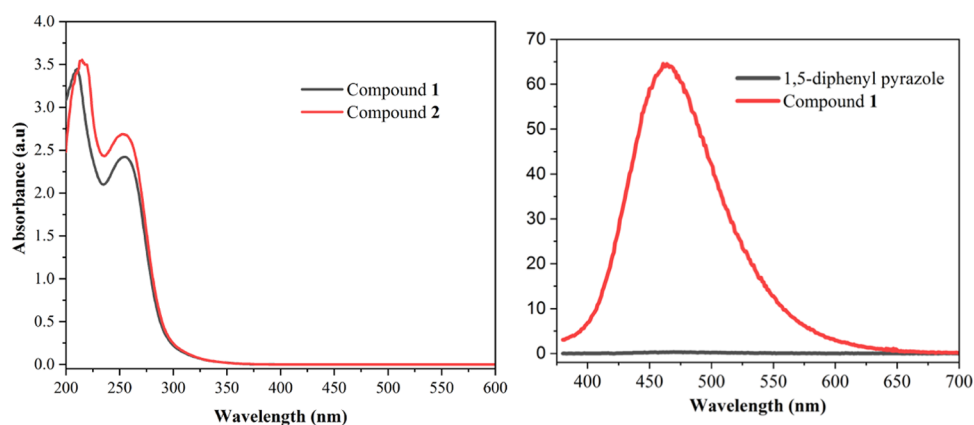
Figure 7. Left: electronic absorption spectra of compounds **1** and **2** in DMF. Right: emission spectra of compound **1** and the concerned ligand in DMF at room temperature.
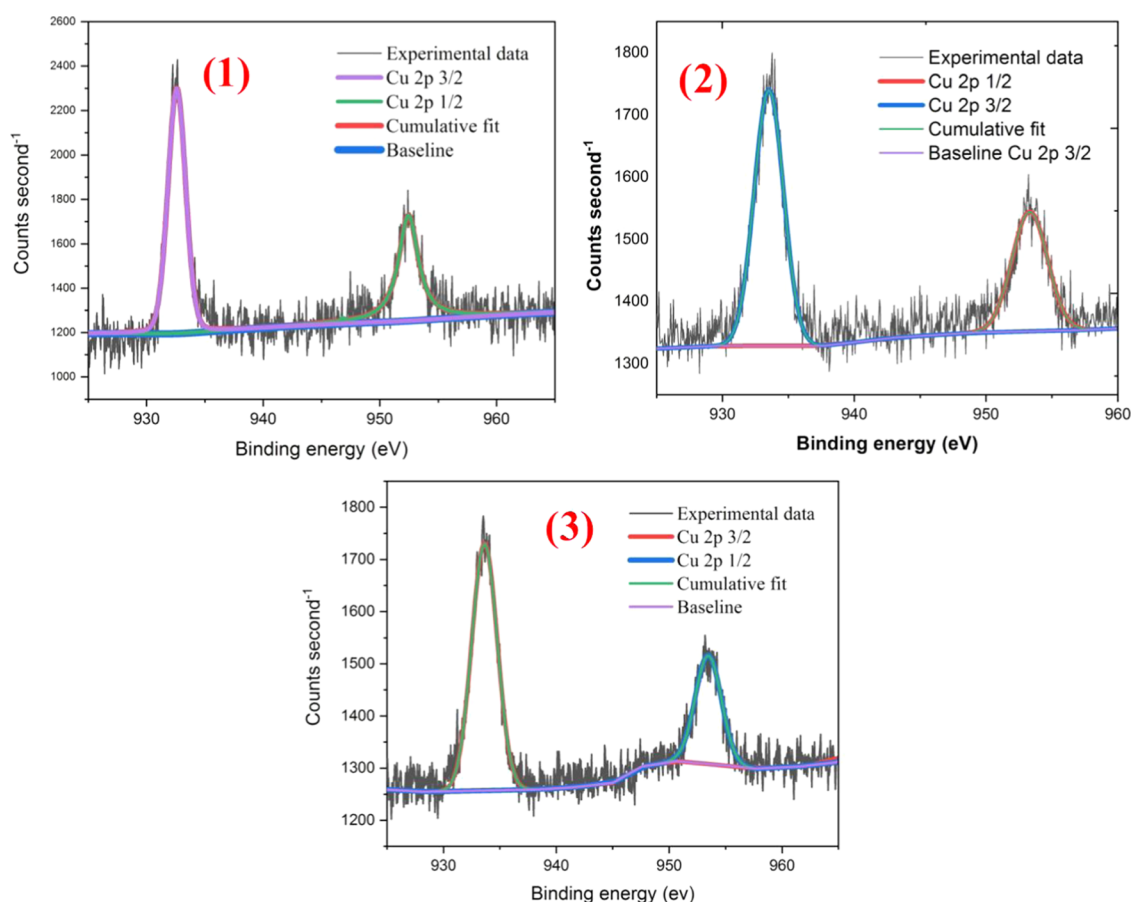

Figure 8. XPS plots showing the presence of Cu(I) (∼932.44 and ∼952.40 eV) in compounds **1**−**3**.

compound **1** are also analyzed in a DMF solution. As shown in the emission spectra (Figure 7 right), the directly synthesized ligand 1,5-diphenylpyrazole *per se* does not show emission, while the same ligand coordinated to Cu(I) in complex **1** is highly emissive in the DMF solution when excited at 270 nm.

Thus, the present system is very unique in the sense that generally, the emission of an organic ligand gets quenched when it forms a coordination complex with a transition metal ion, but in the present work, it is the other way around. This work would have an impact in related biological systems.

The oxidation state of Cu(I) is confirmed from the XPS measurements of compounds **1**−**3**. The XPS plots for copper

are given in Figure 8, and the oxidation state Cu(I) is evident from the binding energies at ∼952.40 eV ($2p_{1/2}$) and ∼932.44 eV ($2p_{3/2}$). The XPS plots for tungsten, carbon, oxygen, nitrogen, and phosphorus are given in Figures S19−S21 in the Supporting Information. The binding energies for other constituent elements of compound **1** are as follows: C_{1s} (∼283.5 eV), N_{1s} (∼398.0 eV), O_{1s} (∼531.0 eV), and P_{2p} (∼133.5, ∼135.3 eV) The binding energy of W(VI) is at ∼31.80 eV ($4f_{7/2}$). Compound **2** exhibits the binding energies corresponding to C_{1s} (284 eV), N_{1s} (∼402 eV), O_{1s} (∼531.0 eV), and P_{2p} (∼133.5, ∼135.3 eV). The binding energies corresponding to Cu(I) are ∼952.40 eV ($2p_{1/2}$) and 932.44 eV
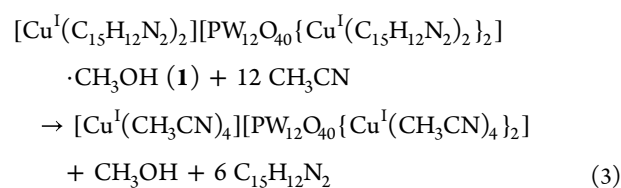
($2p_{3/2}$). The binding energies at 31.80 eV ($4f_{7/2}$) and 34 eV ($4f_{5/2}$) correspond to W(VI) in compound **2**. Compound **3** shows the binding energy values that correspond to C_{1s} (~285.0 eV), N_{1s} (~400.0 eV), O_{1s} (~531.0 eV), and P_{2p} (~133.5 and ~135.3 eV). The binding energies at 952.0 eV ($2p_{1/2}$) and ~934.0 eV ($2p_{3/2}$) correspond to the Cu(I) oxidation state. The W(VI) is evident from the binding energies of ~36.0 eV ($4f_{7/2}$) and ~38.5 eV ($4f_{5/2}$) in compound **3**. The XPS plots for the remaining elements of compounds **1**−**3** are provided in the Supporting Information.

High-resolution mass spectroscopy (HRMS) for all the compounds **1**−**3** was performed in a dimethyl sulfoxide (DMSO) solvent, and the data were collected in the positive ion mode. The HRMS plots are shown in the Supporting Information (section 18). The major m/z peak which is common in the electrospray ionization (ESI) mass spectra of all three compounds is 503, which can be assigned to the $[Cu^I(C_{15}H_{12}N_2)_2]^+$ fragment. We attempted to assign other m/z peaks for the compounds by consulting with the relevant literature,[45,46] e.g., the m/z peak at 947 can be assigned to the fragment $\{H_3W_4O_{13}\}^+$, the m/z peak at 1087 can be assigned to the fragment $\{H_2 CuPW_4O_{16}\}^+$, and the m/z peak at 1177 can be assigned to the fragment $\{H_3W_5O_{16}\}^+$. We could not assign some of the m/z peaks found in the ESI mass spectra.

DFT Calculations. To understand the enormous stability of the present Cu(I) system toward oxidation, we performed DFT calculations[47] of compound **1**. Based on the theoretical calculations, we have observed that upon coordination of the pyrazole ligand with the Cu(I) ion, the highest occupied molecular orbital (HOMO)−lowest unoccupied molecular orbital (LUMO) gap of the coordinated system gets decreased (Figure S9), which implies a feasible metal-to-ligand charge transfer (MLCT). An effective charge transfer requires a lower energy gap between the HOMO and the LUMO, which actually occurs in the present system. This facilitates the donation of π-electron density of the Cu(I) center to the antibonding orbitals of the pyrazole ligand (Figure S10). This explains why the present Cu(I) system cannot be oxidized by oxygen in the present study.

Also, the Mulliken atomic charge distributions show that there is an increase in the electron density at the N atom when the Cu(I) metal ion coordinates with the ligand. To quantify this effect, the values of the Mulliken atomic charge distributions are shown in Figure S10, which exhibit the change from −0.155 to −0.372.

Synthesis Impact of Compound 1 in Organic Synthesis. The gas chromatogram of compound **1** has been compared with that of cinnamaldehyde phenylhydrazone and 1,5 diphenylpyrazole ligands (synthesized separately with the reported procedure)[48] as shown in Figures S9−S11. Typically, compound **1** was dissolved in an acetonitrile solvent, and gas chromatography (GC) analysis was carried out. When acetonitrile solution of compound **1** was run through GC, it gives the GC trace of the 1,5-diphenylpyrazole ligand. This means that when compound **1** is dissolved in acetonitrile, the acetonitrile solvent coordinates to the Cu(I) center, replacing the pyrazole ligand as shown in the following reaction.

$$[Cu^I(C_{15}H_{12}N_2)_2][PW_{12}O_{40}\{Cu^I(C_{15}H_{12}N_2)_2\}_2]$$
$$\cdot CH_3OH \text{ (1)} + 12 \text{ } CH_3CN$$
$$\rightarrow [Cu^I(CH_3CN)_4][PW_{12}O_{40}\{Cu^I(CH_3CN)_4\}_2]$$
$$+ CH_3OH + 6 \text{ } C_{15}H_{12}N_2 \qquad (3)$$

The formation of a stable tetrakis(acetonitrile) copper(I), $Cu^I(CH_3CN)_4$ complex is well known validating the above-mentioned reaction (eq 3). This reaction implies that the oxidative cyclization of cinnamaldehyde phenylhydrazone to 1,5-diphenylpyrazole, thereby the synthesis of 1,5-diphenylpyrazole from cinnamaldehyde phenylhydrazone, can be achieved through the synthesis of compound **1**.

■ CONCLUSIONS

This work has several viewpoints. When an organic ligand, cinnamaldehyde phenylhydrazone, is used with a methanolic Cu(II) salt in the presence of a Keggin polyoxometalate (POM), it undergoes oxidative cyclization to 1,5-diphenylpyrazole with concomitant reduction of Cu(II) to Cu(I), resulting in the formation of a system of POM-supported Cu(I)−pyrazole coordination complexes, $[Cu^I(C_{15}H_{12}N_2)_2]$-$[PW_{12}O_{40}\{Cu^I(C_{15}H_{12}N_2)_2\}_2]\cdot CH_3OH$ (**1**). Compound **1** can be described as an organometallic analogue (even though there is no Cu−C bond in it), in the sense that the cyclized ligand 1,5-diphenylpyrazole stabilizes the Cu(I) center so intensely that the Cu(I) center of compound **1** cannot be oxidized, even by heating the compound **1** in air. The unusual stability of compound **1** toward oxygen can be explained by the presence of low-lying molecular orbitals that can accommodate electron density from the Cu(I) center, as obtained from DFT calculations. When an aqueous suspension of compound **1** crystals (compound **1** is water-insoluble) is exposed to pure oxygen, it isomerizes to the compound $[Cu^I(C_{15}H_{12}N_2)_2]_3[PW_{12}O_{40}]$ (**3**) by breaking the Cu−O(POM) coordinate covalent bonds. If compound **1** crystals are treated with the acetonitrile solvent, it loses the ligand, 1,5-diphenylpyrazole, as evidenced from GC studies. Thus, the present system has the potential to offer an organic transformation of cinnamaldehyde phenylhydrazone to 1,5-diphenylpyrazole under ambient conditions. Overall, in a single system, we have demonstrated an unusually stable Cu(I) mononuclear complex that exhibits geometrical isomerization in a transformation and organic transformation under ambient conditions. Even though the pyrazole ligand itself is not emissive, its copper(I) coordination complex coordinated to the POM cluster is emissive at room temperature. This again adds to the importance of the present system in contemporary inorganic chemistry.

■ EXPERIMENTAL SECTION

General Information. Phosphotungstic acid hydrate, cupric acetate, trans-cinnamaldehyde, phenylhydrazine, methanol, acetone, acetonitrile, diethyl ether, and other chemicals were used as procured from traders and were of analytical quality. 1,5-diphenylpyrazole has been synthesized by the following reported procedure for GC analysis.[48] The crystal data were collected by mounting the crystal on a loop using paratone oil. X-ray reflections were acquired on a Bruker-D8 Quest diffractometer instrument having a preinstalled Cryosystems-800 low-temperature setup functioning at a temperature of 99.75 K and a complementary metal oxide

semiconductor (CMOS) detector using Mo Kα radiation, generated from a microfocus sealed tube (50 kV, 1 mA). Data were measured using φ and ω-scans of 0.50° per frame for 100.0 s. Unit cell determination and data collection were performed with the help of APEX2 (Bruker version: 2014.3-0) software. Unit cell parameters were obtained and refined with the program Bruker SAINT (V8.34A). Data reduction was done with Bruker SAINT (V8.34A). All the crystallographic structures were deduced by a direct method, and the SHELXL-2018 version was used for the refinement purpose using the full matrix (least on F^2). All non-H atoms have been refined anisotropically, and positions were obtained using the riding model. For complexes **1** and **3**, several atoms in a polyoxometalate unit were found to be disordered. These atoms (O10, O4, O8, O21, O55, O42, W5, and W12 in **1** and O10 and O50 in **3**) are fixed at two positions using the part command. Moreover, some of the residual electron density in **1** could not be resolved and therefore squeezed[49] using solvent masking software "PLATON". The recovered electron count can be correlated with the disordered lattice methanol and water molecules. Fourier transform infrared (FT-IR) spectra were recorded on a Shimadzu FT-IR spectrometer instrument. Solid-state samples were characterized using the attenuated total reflection mode. We have also performed the background scan of the air before recording the spectra of the compounds. All powder compounds were characterized by powder X-ray diffraction using Cu Kα1 radiation (λ = 1.54059 Å) in the range of 5–40° (2θ) with 2°/min scan rate performed on a Rigaku (miniflex-600) X-ray powder diffractometer functioning in Bragg–Brentano geometry. The sample was prepared on a glass sample holder by overlaying finely divided powder of compounds. UV–vis analysis was performed on a Shimadzu UV–vis spectrophotometer (model: UV 2600) in the wavelength window of 220–800 nm. Fluorescence study was performed with a Cary eclipse Varian, fluorescence spectrophotometer. Room temperature ^{1}H NMR spectra were recorded on a Bruker Advance III operating on 500 MHz. The NMR data were recorded in a d_6-DMSO solvent. Chemical shifts have been shown as δ values relative to tetramethyl silane (TMS), which is used as an internal standard. The gas analysis was carried out using a GC-flame ionization detection (FID) on Shimadzu 2014 GC instrument using an online GC system. Nitrogen was used as a carrier gas. The XPS data for compounds **1–3** were obtained using an Al Kα X-ray source of 1486.7 eV energy on an Omicron electron spectroscopy for chemical analysis (ESCA) instrument (Oxford Instrument Germany). The thermogravimetric analysis (TGA) data were collected on a Mettler-Toledo (model TGA 1) with a preinstalled Minichiller MT/230 in the temperature window of 25–700 °C at the scale of 5 °C/min providing dry nitrogen gas with the flow rate of 20 cm^3/min. Prior to recording the data for the solid sample, a blank experiment was run with the same parameters using an empty ceramic crucible. The data were analyzed using STARe software V13.00. All the electrochemical studies were recorded on a single-channel electrochemical analysis (Autolab-AUT-Metrohm) instrument. The high-resolution mass spectroscopy (HRMS) for all the compounds was performed on a Maxis 10138 (electrospray ionization (ESI) mass data). The measurement was carried out in the DMSO solvent, and the data were collected in the positive ion mode. The ground-state geometry optimization was carried out in the gas phase at the Becke three-parameter hybrid exchange functional in con-

currence with the Lee–Yang–Parr gradient-corrected correlation function (B3LYP functional) level of density functional theory (DFT), using the 6-311++ G(d,p) basis set for the cyclized ligand and its cuprous complexes. DFT calculations have been performed on all stationary points of the potential energy surface (PES) and studied using Gaussian 09W.

Synthesis of Cinnamaldehyde Phenylhydrazone (L). To the ethanolic solution of cinnamaldehyde (0.133 g, 0.01 mmol), a 10 mL ethanolic solution of phenylhydrazine (0. 113 g, 0.01 mmol) was added dropwise. The color of the solution turns yellow. The progress of the reaction is monitored by thin-layer chromatography. Then, the mixture was stirred at room temperature for 1 h. The yellow precipitate is filtered and washed with hexane. The synthesized ligand is characterized with ^{1}H NMR spectroscopy. Yield = 88%, melting point = 140 °C. 7.51 (s, 1H, N−H) 7.45−7.50 (d, 1H, −CH=N), 7.25−7.42 (5H, Ar-H): cinnamaldehyde, 6.94−7.00 (5H, Ar-H): phenylhydrazine aromatic protons, 6.80−6.83 (t, 1H, −CH=C−) 6.60−6.65 (d, 1H, C=CH−).

Synthesis of [Cu^I(C$_{15}$H$_{12}$N$_2$)$_2$] [PW$_{12}$O$_{40}${Cu^I(C$_{15}$H$_{12}$N$_2$)$_2$}$_2$]· CH$_3$OH (1). Cinnamaldehyde phenylhydrazone (0.020 g, 0.03 mol) is dissolved in 10 mL of 1:1 methanol and water mixture. The resulting solution is stirred for 30 min. The 5 mL aqueous solution of cupric acetate (0.020 g, 0.06 mol) is added to the ligand solution. Furthermore, 5 mL of aqueous phosphotungstic acid solution (0.072 g, 0.01 mol) is added to the reaction mixture. The resulting green-colored reaction mixture is transferred to a teflon beaker of a hydrothermal autoclave. The reaction mixture is heated at 120 °C for 24 h in a hydrothermal oven. Golden yellow crystals of compound **1** suitable for single-crystal X-ray diffraction studies were separated from the reaction mixture. Yield = 33%. Elemental analysis: calculated: C, 25.26; H, 1.79; N, 4.41. Found: C, 24.72; H, 1.73; N, 3.80.

Synthesis of [Cu^I(C$_{15}$H$_{12}$N$_2$)$_2$] [PW$_{12}$O$_{40}${Cu^I(C$_{15}$H$_{12}$N$_2$)$_2$}$_2$] (2). The single crystals of compound **1** were heated at 55 °C under aerial conditions for 5 h. The single crystals of compound 1 are converted into compound **2** by the desolvation of the methanol molecule. Elemental analysis: calculated: C, 25.16; H, 1.67; N, 4.48. Found: C, 24.63; H, 1.65; N, 3.83.

Synthesis of [Cu^I(C$_{15}$H$_{12}$N$_2$)$_2$]$_3$[PW$_{12}$O$_{40}$] (3). A total of 10 mg of compound **1** single crystals is suspended in 10 mL of deionized water, and pure oxygen (99.99%) is bubbled through the suspension for 30 min, resulting in single crystals of compound **3**. Elemental analysis: calculated: C, 24.63; H, 1.45; N, 4.37. Found: C, 25.35; H, 1.70; N, 3.94.

Synthesis of [C$_{15}$H$_{12}$N$_2$] (4). The procedure used for the synthesis of compound **1** is employed here, but cobalt acetate is used instead of copper acetate. Light-yellow-colored single crystals were isolated and characterized using the single-crystal X-ray technique. The single-crystal structure shows the presence of the cyclized 1,5-diphenylpyrazole ligand.

■ ASSOCIATED CONTENT

ⓢ Supporting Information

The Supporting Information is available free of charge at https://pubs.acs.org/doi/10.1021/acsomega.2c03795.

> FT-IR spectroscopic analysis; PXRD; XPS; ESI mass spectrum; thermogravimetric analysis; data collection parameters; tabulated bond lengths and bond angles for the X-ray crystallography; additional figures to support

the discussion of the spectroscopic properties of the complexes; and additional figures and tables to support the discussion of the DFT calculations (PDF)

Accession Codes

The CCDC numbers for compounds **1**, **2**, and **3** are 2122528, 2122529, and 2122530, respectively. The CCDC number for the molecular compound 1,5-diphenylpyrazole is 2122531. The supplementary crystallographic data for this paper can be obtained free of charge via www.ccdc.cam.ac.uk/data_request/cif or by emailing data_request@ccdc.cam.ac.uk or by contacting the Cambridge Crystallographic Data Centre, 12 Union Road, Cambridge CB2 1EZ, UK; fax: +44 1223 336033.

■ AUTHOR INFORMATION

Corresponding Author

Sabbani Supriya — *School of Physical Sciences, Jawaharlal Nehru University, New Delhi 110067, India;* ● orcid.org/0000-0002-3644-4506; Phone: +91-11-26738812; Email: ssabbani@mail.jnu.ac.in, sabbani07@gmail.com

Authors

Neeraj Kumar Mishra — *School of Physical Sciences, Jawaharlal Nehru University, New Delhi 110067, India*

Deepak Bansal — *Materials Research and Technology, Luxembourg Institute of Science and Technology, 4362 Esch-sur-Alzette, Luxembourg*

Complete contact information is available at:
https://pubs.acs.org/10.1021/acsomega.2c03795

Author Contributions

The article was written through contributions of all authors. All authors have given approval to the final version of the article.

Notes

The authors declare no competing financial interest.

■ ACKNOWLEDGMENTS

■ REFERENCES

(1) M. T., Pope *Heteropoly and Isopoly Oxometalates*, Springer Verlag: Berlin, 1983.

(2) Pope, M. T.; Müller, A. Polyoxometalate Chemistry: An Old Field with New Dimensions in Several Disciplines. *Angew. Chem., Int. Ed.* **1991**, *30*, 34−48.

(3) Miras, H. N.; Yan, J.; Long, D. L.; Cronin, L. Engineering polyoxometalates with emergent properties. *Chem. Soc. Rev.* **2012**, *41*, 7403−7430.

(4) Keita, B.; Nadjo, L. Electrochemistry of Isopoly and Heteropoly Oxometalates. In *Encyclopedia of Electrochemistry*, Bard, A. J.; Stratmann, M., Eds.; Wiley-VCH, 2006; Vol 7, pp 607−700.

(5) Sadakane, M.; Steckhan, E. Electrochemical Properties of Polyoxometalates as Electrocatalysts. *Chem. Rev.* **1998**, *98*, 219−238.

(6) Clemente-Juan, J. M.; Coronado, E.; Gaita-Ariño, A. Magnetic polyoxometalates: from molecular magnetism to molecular spintronics and quantum computing. *Chem. Soc. Rev.* **2012**, *41*, 7464−7478.

(7) Müller, A.; Peters, F.; Pope, M. T.; Gatteschi, D. Polyoxometalates:Very Large Clusters−Nanoscale Magnets. *Chem. Rev.* **1998**, *98*, 239−272.

(8) Wang, S. S.; Yang, G. Y. Recent Advances in Polyoxometalates-Catalysed Reactions. *Chem. Rev.* **2015**, *115*, 4893−4962.

(9) Riemer, D.; Mandaviya, B.; Schilling, W.; Götz, A. C.; Kühl, T.; Finger, M.; Das, S. CO$_2$-Catalyzed Oxidation of Benzylic and Allylic Alcohols with DMSO. *ACS Catal.* **2018**, *8*, 3030−3034.

(10) Mizuno, N.; Misono, M. Heterogeneous Catalysis. *Chem. Rev.* **1998**, *98*, 199−218.

(11) Hill, C. L. Polyoxometalates in Catalysis. *J. Mol. Catal. A: Chem.* **2007**, *262*, 1−242.

(12) Wang, Q.; Xu, B.; Wang, Y.; Wang, H.; Hu, X.; Ma, P.; Niu, J.; Wang, J. Polyoxometalate-Incorporated Framework as a Heterogeneous Catalyst for Selective Oxidation of C-H Bonds of Alkylbenzenes. *Inorg. Chem.* **2021**, *60*, 7753−7761.

(13) Vasylyev, M. V.; Neumann, R. New Heterogeneous Polyoxometalate Based Mesoporous Catalysts for Hydrogen Peroxide Mediated Oxidation Reactions. *J. Am. Chem. Soc.* **2004**, *126*, 884−890.

(14) Neumann, R.; Khenkin, A. M. Molecular oxygen and oxidation catalysis by phosphovanadomolybdates. *Chem. Commun.* **2006**, 2529−2538.

(15) Dolbecq, A.; Dumas, E.; Mayer, C. R.; Mialane, P. Hybrid organic−inorganic polyoxometalate compounds: from structural diversity to applications. *Chem. Rev.* **2010**, *110*, 6009−6048.

(16) Pradeep, C. P.; Long, D. -L.; Cronin, L. Cations in control: crystal engineering polyoxometalate clusters using cation directed self-assembly. *Dalton Trans.* **2010**, *39*, 9443−9457.

(17) Proust, A.; Thouvenot, R.; Gouzerh, P. Functionalization of polyoxometalates: towards advanced applications in catalysis and materials science. *Chem. Commun.* **2008**, 1837−1852.

(18) Proust, A.; Matt, B.; Villanneau, R.; Guillemot, G.; Gouzerh, P.; Izzet, G. Hybrid polyoxometalates as post-functionalization platforms: from fundamentals to emerging applications. *Chem. Soc. Rev.* **2012**, *41*, 7605−7622.

(19) Anyushin, A. V.; Aleksandar Kondinski, A.; Parac-Vogt, T. N. Hybrid polyoxometalates as post-functionalization platforms: from fundamentals to emerging applications. *Chem. Soc. Rev.* **2020**, *49*, 382−432.

(20) Kar, A.; Pradeep, C. P. Post-functionalization through covalent modification of organic counter ions: a stepwise and controlled approach for novel hybrid polyoxometalate materials. *Dalton Trans.* **2020**, *49*, 12174−12179.

(21) Zhao, D. C.; Hu, Y. Y.; Ding, H.; Guo, H. Y.; Cui, X. B.; Zhang, X.; Huo, Q. S.; Xu, J. Q. Polyoxometalate based Organic−Inorganic hybrid compounds containing transition metal mixed-organic-ligand complexes of N-containing and pyridine carboxylate ligands. *Dalton Trans.* **2015**, *44*, 8971−8983.

(22) Hu, T. P.; Zhao, Y. Q.; Mei, K.; Lin, S. J.; Wang, X. P.; Sun, D. A novel silver(I)-Keggin-polyoxometalate inorganic−organic hybrid: a Lewis acid catalyst for cyanosilylation reaction. *CrystEngComm* **2015**, *17*, 5947−5952.

(23) Singh, C.; Mukhopadhyay, S.; Das, S. K. Polyoxometalate-Supported Bis(2,2′-bipyridine) mono(aqua)nickel (II) Coordination Complex: An Efficient Electrocatalyst for Water Oxidation. *Inorg. Chem.* **2018**, *57*, 6479−6490.

(24) Santoni, M. P.; Hanan, G. S.; Hasenknopf, B. Covalent multi-component systems of polyoxometalates and metal complexes: Toward multi-functional organic−inorganic hybrids in molecular and material sciences. *Coord. Chem. Rev.* **2014**, *281*, 64−85.

(25) Liu, D. S.; Chen, W. T.; Ye, G. M.; Liu, J. Q.; Sui, Y. Synthesis and characterization of an inorganic-organic hybrid copper coordination polymer based on well-defined Keggin polyanions. *Inorg. Chim. Acta* **2018**, *477*, 84−88.

(26) Wang, X.; Wang, Y.; Liu, G.; Tian, A.; Zhang, J.; Lin, H. Novel inorganic−organic hybrids constructed from multinuclear copper cluster and Keggin polyanions: from 1D wave-like chain to 2D network. *Dalton Trans.* **2011**, *40*, 9299−9305.

(27) Sorrell, T. N.; Malachowski, M. R. Mononuclear three-coordinate copper(I) complexes: synthesis, structure, and reaction with carbon monoxide. *Inorg. Chem.* **1983**, *22*, 1883−1887.

(28) Baranova, K. F.; Titov, A. A.; Smolyakov, A. F.; Chernyadyev, A. Y.; Filippov, O. A.; Shubina, E. S. Mononuclear Copper(I) 3-(2-pyridyl)pyrazole Complexes: The Crucial Role of Phosphine on Photoluminescence. *Molecules* **2021**, *26*, 6869.

(29) Chen, J. L.; Cao, X. F.; Wang, J. Y.; He, L. H.; Liu, Z. Y.; Wen, H. R.; Chen, Z. N. Synthesis, Characterization, and photophysical properties of heteroleptic copper(I) complexes with functionalized 3-(20-pyridyl)-1,2,4-triazole chelating ligands. *Inorg. Chem.* **2013**, *52*, 9727−9740.

(30) Zhang, Q.; Chen, X. L.; Chen, J.; Wu, X. Y.; Yu, R.; Lu, C. Z. Four highly efficient cuprous complexes and their applications in solution processed organic light-emitting diodes. *RSC Adv.* **2015**, *5*, 34424−34431.

(31) Chen, J. L.; Guo, Z. H.; Yu, H. G.; He, L. H.; Liu, S. J.; Wen, H. R.; Wang, J. Y. Luminescent dinuclear copper(I) complexes bearing 1,4-bis(diphenylphosphino)butane and functionalized 3-(20-pyridyl)-pyrazole mixed ligands. *Dalton Trans.* **2016**, *45*, 696−705.

(32) Chen, J. L.; Guo, Z. H.; Luo, Y. S.; Qiu, L.; He, L. H.; Liu, S. J.; Wen, H. R.; Wang, J. Y. Luminescent monometallic Cu(I) triphenylphosphine complexes based on methylated 5-trifluoromethyl-3-(2-pyridyl)-1,2,4-triazole ligands. *New J. Chem.* **2016**, *40*, 5325−5332.

(33) Sun, Y.; Lemaur, V.; Beltran, J. I.; Cornil, J.; Huang, J.; Zhu, J.; Wang, Y.; Frohlich, R.; Wang, H.; Jiang, L.; Zou, G. Neutral Mononuclear Copper(I) Complexes: Synthesis, Crystal Structures, and Photophysical Properties. *Inorg. Chem.* **2016**, *55*, 5845−5852.

(34) He, L. H.; Luo, Y. S.; Di, B. S.; Chen, J. L.; Ho, C. L.; Wen, H. R.; Liu, S. J.; Wang, J. Y.; Wong, W. Y. Luminescent Three- and Four-Coordinate Dinuclear Copper(I) Complexes Triply Bridged by Bis(diphenylphosphino)methane and Functionalized 3-(20 -Pyridyl)-1,2,4-triazole Ligands. *Inorg. Chem.* **2017**, *56*, 10311−10324.

(35) Donato, L.; Atoini, Y.; Prasetyanto, E. A.; Chen, P.; Rosticher, C.; Bizzarri, C.; Rissanen, K.; De, C. L. Selective Encapsulation and Enhancement of the Emission Properties of a Luminescent Cu(I) Complex in Mesoporous Silica. *Helv. Chim. Acta* **2018**, *101*, No. e1700273.

(36) For recent reviews on C−N bond formations, see: (a) Alberico, D.; Scott, M. E.; Lautens, M. Aryl−Aryl Bond Formation by Transition-Metal-Catalyzed Direct Arylation. *Chem. Rev.* **2007**, *107*, 174−238. (b) Surry, D. S.; Buchwald, S. L. Dialkylbiaryl phosphines in Pd-catalyzed amination: a user's guide. *Chem. Sci.* **2011**, *2*, 27−50. (c) Cho, S. H.; Kim, J. Y.; Kwak, J.; Chang, S. *Chem. Soc. Rev.* **2011**, *40*, 5068−5083.

(37) Li, X.; Li, H.; Chen, H.; Wu, W.; Jiang, H. Copper-Catalyzed Aerobic $C(sp^2)$−H Functionalization for C−N Bond Formation: Synthesis of Pyrazoles and Indazoles. *J. Org. Chem.* **2013**, *78*, 3636−3646.

(38) Neumann, J. J.; Suri, M.; Glorius, F. Efficient Synthesis of Pyrazoles: Oxidative C−C/N−N Bond-Formation Cascade. *Angew. Chem., Int. Ed.* **2010**, *49*, 7790−7794.

(39) For reports on reductive elimination of N-arylamines or N-arylimines from the putative aminyl or iminyl copper (III) species, see: (a) Zhou, W.; Liu, Y.; Yang, Y.; Deng, G. J. Copper-catalyzed intramolecular direct amination of sp^2 C−H bonds for the synthesis of N-aryl acridones. *Chem. Commun.* **2012**, *48*, 10678−10680. (b) Liu, S.; Yu, Y.; Liebeskind, L. S. N-Substituted Imines by the Copper-Catalyzed N-Imination of Boronic Acids and Organostannanes with O-Acyl Ketoximes. *Org. Lett.* **2007**, *9*, 1947−1950. (c) Guru, M. M.; Ali, M. A.; Punniyamurthy, T. Copper(II)-Catalyzed Conversion of Bisaryloxime Ethers to 2-Arylbenzoxazoles via C−H Functionalization/C−N/C−O Bonds Formation. *Org. Lett.* **2011**, *13*, 1194−1197.

(40) (a) *SAINT*. Bruker AXS Inc: Madison, Wisconsin, USA, 2013. (b) *SAINT*. Bruker AXS Inc.: Madison, Wisconsin, USA, 2012.

(41) Sheldrick, G. M. *SHELXTL*, version 2014/7. http://shelx.uniac.gwdg.de/SHELX/index.php.

(42) O'Keefe, M.; Brese, N. E. Atom sizes and bond lengths in molecules and crystals. *J. Am. Chem. Soc.* **1991**, *113*, 3226−3229.

(43) Lin, J.; Wang, N.; Chen, X.; Yang, X.; Hong, L.; Ruan, Z.; Ye, H.; Chen, Y.; Lian, X. Electrocatalytic water oxidation by copper(II) complexes with a pentadentate amine-pyridine ligand. *Sustainable Energy Fuels* **2022**, *6*, 1312−1318.

(44) Shakeela, K.; Dithya, A. S.; Rao, C. J.; Rao, G. R. Electrochemical behaviour of Cu(II)/Cu(I) redox couple in 1-hexyl-3-methylimidazolium chloride ionic liquid. *J. Chem. Sci.* **2015**, *127*, 133−140.

(45) Vilà-Nadal, L.; Mitchell, S. G.; Antonio Rodrı́guez-Fortea, A.; Miras, H. N.; Cronin, L.; Poblet, J. M. Connecting theory with experiment to understand the initial nucleation steps of hetero-polyoxometalate clusters. *Phys. Chem. Chem. Phys.* **2011**, *13*, 20136−20145.

(46) Ma, M. T.; Waters, T.; Karin Beyer, K.; Palamarczuk, R.; Richardt, P. J. S.; O'Hair, R. A. J.; Wedd, A. G. Gas-Phase Fragmentation of Polyoxotungstate Anions. *Inorg. Chem.* **2009**, *48*, 598−606.

(47) Frisch, M. J.; Trucks, G. W.; Schlegel, H. B.; Scuseria, G. E.; Robb, M. A.; Cheeseman, J. R.; Scalmani, G.; Barone, V.; Mennucci, B.; Petersson, G. A.; Nakatsuji, H.; Caricato, M.; Li, X.; Hratchian, H. P.; Izmaylov, A. F.; Bloino, J.; Zheng, G.; Sonnenberg, J. L.; Hada, M.; Ehara, M.; Toyota, K.; Fukuda, R.; Hasegawa, J.; Ishida, M.; Nakajima, T.; Honda, Y.; Kitao, O.; Nakai, H.; Vreven, T.; Montgomery, J. A., Jr.; Peralta, J. E.; Ogliaro, F.; Bearpark, M.; Heyd, J. J.; Brothers, E.; Kudin, K. N.; Staroverov, V. N.; Kobayashi, R.; Normand, J.; Raghavachari, K.; Rendell, A.; Burant, J. C.; Iyengar, S. S.; Tomasi, J.; Cossi, M.; Rega, N.; Millam, J. M.; Klene, M.; Knox, J. E.; Cross, J. B.; Bakken, V.; Adamo, C.; Jaramillo, J.; Gomperts, R.; Stratmann, R. E.; Yazyev, O.; Austin, A. J.; Cammi, R.; Pomelli, C.; Ochterski, J. W.; Martin, R. L.; Morokuma, K.; Zakrzewski, V. G.; Voth, G. A.; Salvador, P.; Dannenberg, J. J.; Dapprich, S.; Daniels, A. D.; Farkas, Ö.; Foresman, J. B.; Ortiz, J. V.; Cioslowski, J.; Fox, D. J. *Gaussian 09*, revision D.01; Gaussian, Inc.: Wallingford CT, 2009.

(48) Zhang, X.; Kang, J.; Niu, P.; Wu, J.; Yu, W.; Chang, J. I_2-Mediated Oxidative C−N Bond Formation for Metal-Free One-Pot Synthesis of Di-, Tri-, and Tetrasubstituted Pyrazoles from $α$, $β$-Unsaturated Aldehydes/Ketones and Hydrazines. *J. Org. Chem.* **2014**, *79*, 10170−10178.

(49) Spek, A. L. *PLATON, A Multipurpose Crystallographic Tool*, version 160617; Utrecht University: The Netherlands.